Journal of Maps
Publication details, including instructions for authors and subscription information:
http://www.tandfonline.com/loi/tjom20

Glacial geomorphology of the Shaluli Shan area, southeastern Tibetan Plateau

Ping Fu [a b], Jakob Heyman [a], Clas Hättestrand [b], Arjen P. Stroeven [b] & Jonathan M. Harbor [a]

[a] Department of Earth and Atmospheric Sciences, Purdue University, IN-47907, West Lafayette, USA

[b] Department of Physical Geography and Quaternary Geology, Stockholm University, SE-106 91, Stockholm, Sweden

Available online: 28 Mar 2012

Journal of Maps
2012, 1–8, iFirst Article

SCIENCE

Glacial geomorphology of the Shaluli Shan area, southeastern Tibetan Plateau

Ping Fu[a,b]*, Jakob Heyman[a], Clas Hättestrand[b], Arjen P. Stroeven[b] and Jonathan M. Harbor[a]

[a]*Department of Earth and Atmospheric Sciences, Purdue University, IN-47907, West Lafayette, USA;* [b]*Department of Physical Geography and Quaternary Geology, Stockholm University, SE-106 91, Stockholm, Sweden*

(*Received 16 August 2011; Revised 12 February 2012; Accepted 16 February 2012*)

We present a glacial geomorphological map covering 1.04×10^5 km^2 of the Shaluli Shan (Shan = Mountain), southeastern Tibetan Plateau. Using a 90 m digital elevation model from the Shuttle Radar Topography Mission and 15/30 m Landsat Enhanced Thematic Mapper Plus satellite imagery, we have mapped glacial valleys, marginal moraines, hummocky terrain, glacial lineations and ice-scoured terrain. Lineations and scoured areas largely overlap on the low relief granite plateau of the Shaluli Shan and relate to former ice cap glaciation. These landscape features indicate that past ice cap glaciation included basal sliding conditions, and thus warm-based ice. Glacial valleys and marginal moraines are dominant landforms in the high mountain ranges of Shaluli Shan and occur on and fringing the plateau. This glacial geomorphological map forms the basis for paleoglaciological reconstructions of this southeastern Tibetan Plateau region and indicates the former presence of multiple glaciations involving valley glaciers and ice caps. The map is presented at a scale of 1:630,000.

Keywords: glacial geomorphology; glaciation; landform; ice cap; Tibetan Plateau; Shaluli Shan; glacial valley; moraine; lineations; ice-scoured terrain

1. Introduction

Reconstructing the extent, timing and geologic impact of Tibetan Plateau glaciation is important because of the central role of glaciation in paleoclimate reconstructions and geologic evolution models. Considerable controversy surrounds past paleoglaciological reconstructions of the Tibetan Plateau that range from a plateau-wide ice sheet synchronous with northern hemisphere glaciation (Kuhle, 1988) to limited glacier and ice cap expansions with timing and extents that do not match the northern hemisphere record (e.g., Lehmkuhl & Owen, 2005; Owen et al., 2005; Rutter, 1995; Zhou, Li, Zhang, Zhao, & Cui, 2004). Although past glaciations have been reconstructed for some regions (e.g., Heyman et al., 2011; Owen et al., 2005), and the hypothesis of a plateau-wide ice sheet during the last glacial maximum has been rejected (e.g., Heyman et al., 2009; Li et al., 1991), the extent and timing of glaciation in many areas remains poorly documented.

Detailed glacial landform maps allowing reconstructions of regional glaciations (Figure 1) have been presented for Bayan Har Shan (Heyman, Hättestrand, & Stroeven, 2008) and Tanggula Shan (Morén, Heyman, & Stroeven, 2011). This paper extends the Tibetan glacial landform mapping effort to the Shaluli Shan.

The Shaluli Shan is largely ice free today, but includes features of Alpine glaciation commonly observed in the high mountain ranges of the Tibetan Plateau. Previous work in this region has identified glacial landforms (Li et al., 1991; Xu & Zhou, 2009; Zheng & Ma, 1995) and provided chronological control (Graf et al., 2008; Schäfer et al., 2002; Strasky et al., 2009; Wang, Raisbeck, Xu, Yiou, & Ba, 2006; Xu & Zhou, 2009), but a detailed yet comprehensive mapping of the geomorphology to underpin paleoglaciological reconstructions is lacking. The mapping work presented in this paper, together with forthcoming results on glacial chronology are aimed at improving our understanding of the paleoglaciology of the Shaluli Shan and the southeastern Tibetan Plateau.

*Corresponding author. Email: ping.fu@natgeo.su.se

ISSN 1744-5647 online

http://dx.doi.org/10.1080/17445647.2012.668762
http://www.tandfonline.com

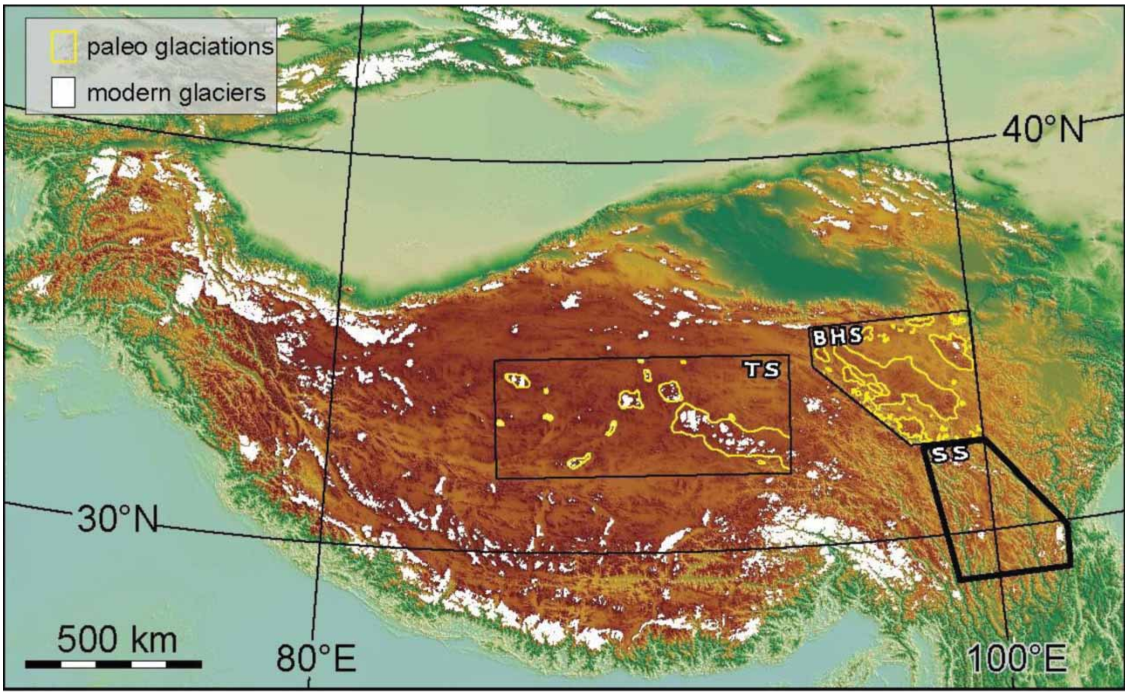

Figure 1. Detailed glacial landform maps covering large regions ($>10^5$ km^2) of the Tibetan Plateau. Paleoglaciological reconstructions (shown in yellow) are the minimum extents of maximum glaciation proposed by Morén et al. (2011) for Tanggula Shan (TS) and Heyman et al. (2009) for Bayan Har Shan (BHS) of the central and northeastern Tibetan Plateau, respectively. Modern glacier extent (white) is derived from GLIMS (http://www.glims.org). The map presented in this study covers the Shaluli Shan (SS) on the southeastern margin of the Tibetan Plateau.

Figure 2. Google Earth image looking east across the Haizishan plateau within the Shaluli Shan. The large number of lakes (A) on the low-relief plateau is indicative of glacial scouring, and the pattern of lineations (B) is indicative of ice cap glaciation with active basal erosion. Close-up images of A and B are shown in Figure 7e and d, respectively.

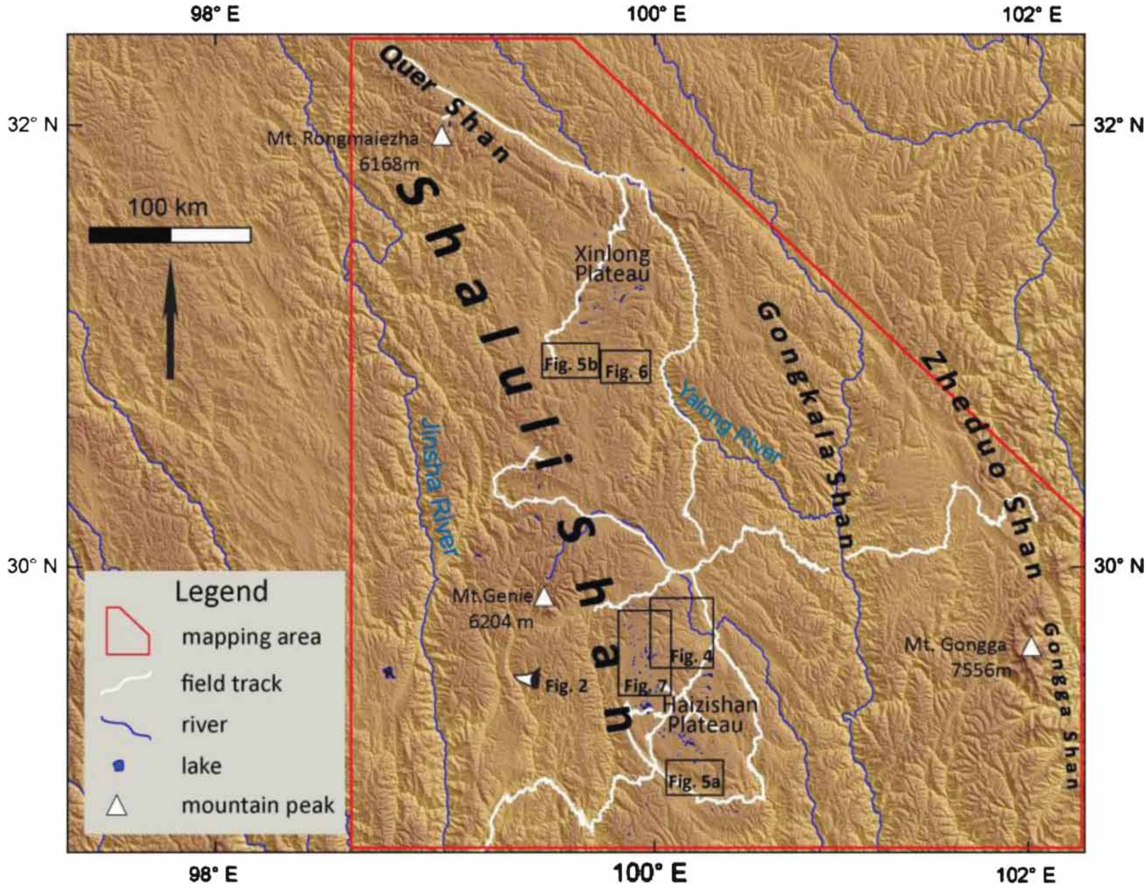

Figure 3. Geography and topography of the study area, including the locations of Figures 2, 4, 5, 6 and 7. DEM from Jarvis, Reuter, Nelson, and Guevara (2008), water bodies from United States Geological Survey (http://www.usgs.gov/), and rivers from National Geomatics Center of China (http://ngcc.sbsm.gov.cn/english/about.asp).

2. Physiography of the Shaluli Shan area

The study area is centered on the Shaluli Shan, southeastern Tibetan Plateau, between the Jinsha River and Yalong River, two of the main branches of Chang Jiang (Figure 3). The Shaluli Shan upland extends north-south, parallel to other regional uplands, and fault-block basins dominate the geologic structure. The bedrock consists mainly of granite, limestone, sandy slate and phyllite (Burchfiel, Chen, Liu, & Royden, 1995). Elevations generally range between 4000 and 5000 m a.s.l., with the highest peak, Mt. Gongga, at 7556 m a.s.l. (Figures 2 and 3). The mapping area extends east to include the Zheduo Shan, forming the topographic margin of the southeastern Tibetan Plateau, and covers 1.04×10^5 km^2 of high mountains and relatively-low relief granite plateaus (e.g., Haizishan and Xinlong plateaus; Figures 2 and 3), surrounded by steep and deep fluvial valleys (cf. Stroeven et al., 2009).

3. Methods

We have mapped glacial landforms using the Shuttle Radar Topography Mission (SRTM) digital elevation model (DEM) with 90 m horizontal resolution (Jarvis et al., 2008), and orthorectified Landsat Enhanced Thematic Mapper Plus (ETM+) imagery (GLCF, 2011) with composites of bands 5, 4, 2 and 4, 3, 2 (30 m resolution) draped with a semi-transparent gray-scale image of band 8 at 15 m resolution. Mapping was primarily performed in ArcGIS 9.3. Google Earth was used for 3D landform visualization and also used to map landforms; mapped polygons were saved as KML file and then converted to a Shapefile using the Data Interoperability toolbox in ArcGIS. The mapped geomorphology has been field-checked in selected areas during 2008 and 2009 (see Figure 3 for tracks along which field checking was performed).

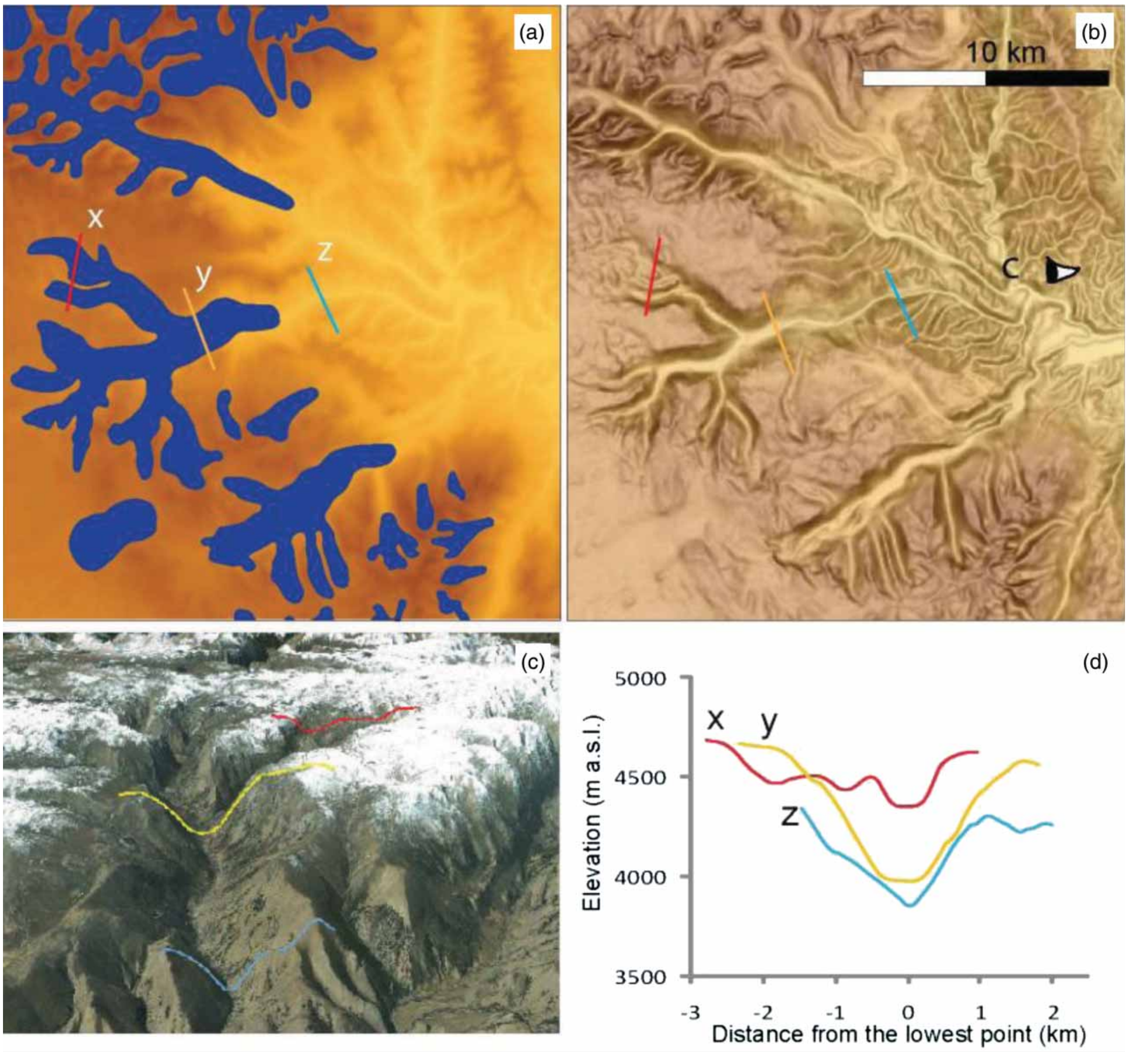

Figure 4. Glacial valleys (a) as mapped features in a colored DEM, (b) on a DEM draped by a semi-transparent greyscale slope image, (c) in a Google Earth view and (d) as cross section profiles (x, y). The locations of cross section profiles x, y (glacial valleys) and z (fluvial valley) are shown in panel (a). The orientation of the Google Earth view (c) is illustrated with an eye in panel b. Location of the area depicted is indicated in Figure 3.

4. Landform definitions and descriptions

4.1 *Glacial valley*

A glacial valley is identified by several features; most notably its U-shaped cross section and smooth valley sides due to the erosion and truncation of interlocking valley spurs (Figure 4). In contrast, valleys formed by fluvial incision typically exhibit V-shaped cross sections and interlocking spurs (Figure 4). In many cases, the highest elevation of former glacial erosion in glacial valleys is represented by an abrupt change in slope that can be identified from the SRTM DEM and Google Earth. Outlet valleys without cirques at their heads surround the two plateaus. The glacial valleys are up to 45 km long, usually less than 3 km wide, and 100–400 m deep (with some 600–700 m deep). A total of 2678 glacial valley polygons were mapped, covering an area of 1.5×10^4 km^2, or about 14% of the total area.

4.2 *Marginal moraines*

Marginal moraines are ridge-shaped constructional landforms created along the margins of glaciers, including arc-shaped moraines and lateral moraines formed by valley or outlet glaciers (Figure 5) and elongated sinuous moraines formed by ice caps. Moraines formed by valley glaciers occur on plains outside valleys, crossing valleys

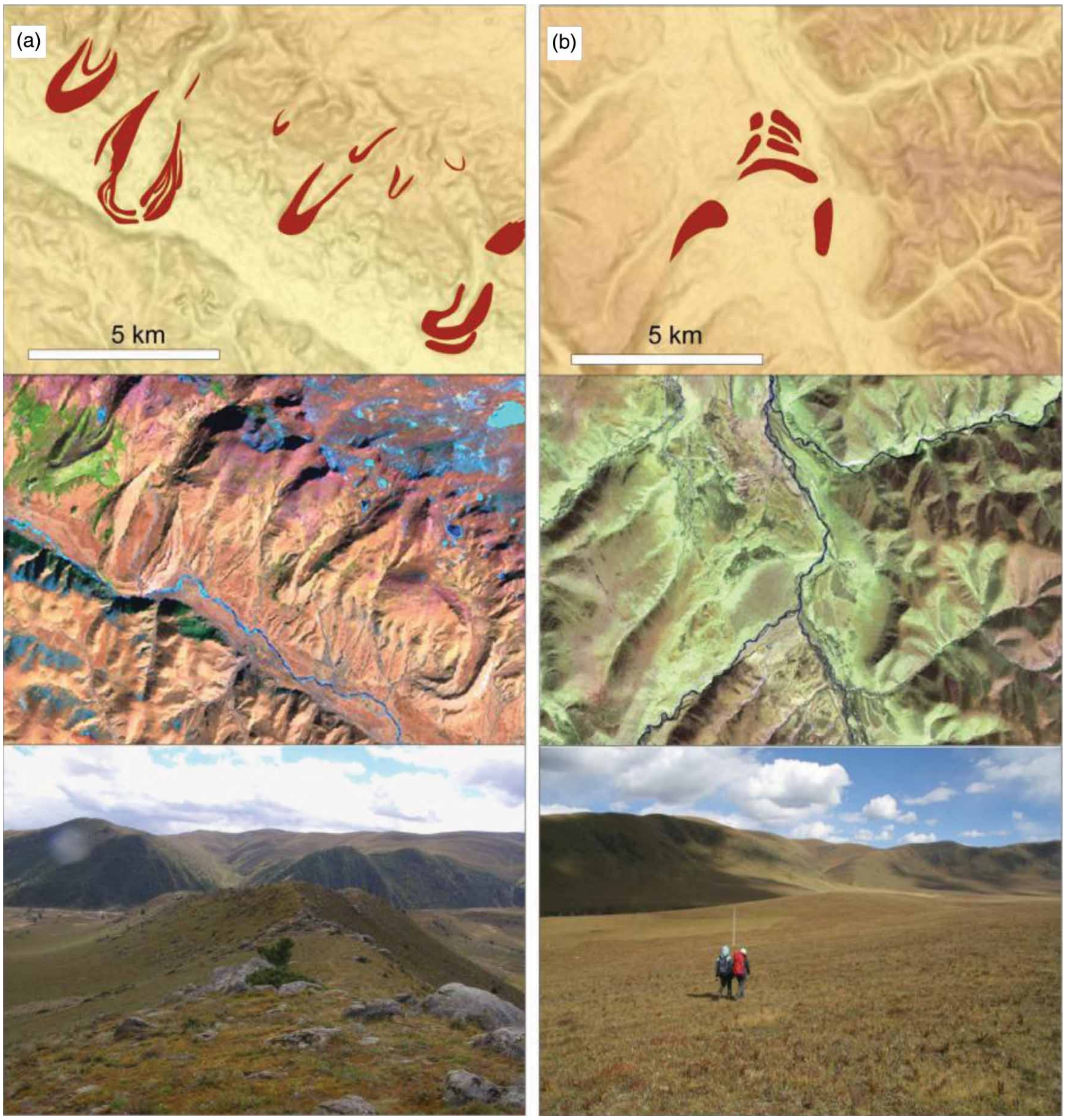

Figure 5. Marginal moraines from (a) Kuzhaori and (b) Nata shown as mapped features on a DEM draped with a semi-transparent slope image (upper panels), Landsat images (middle panels), and photographs taken in the field (lower panels). Locations of panel 5a and 5b are detailed in Figure 3.

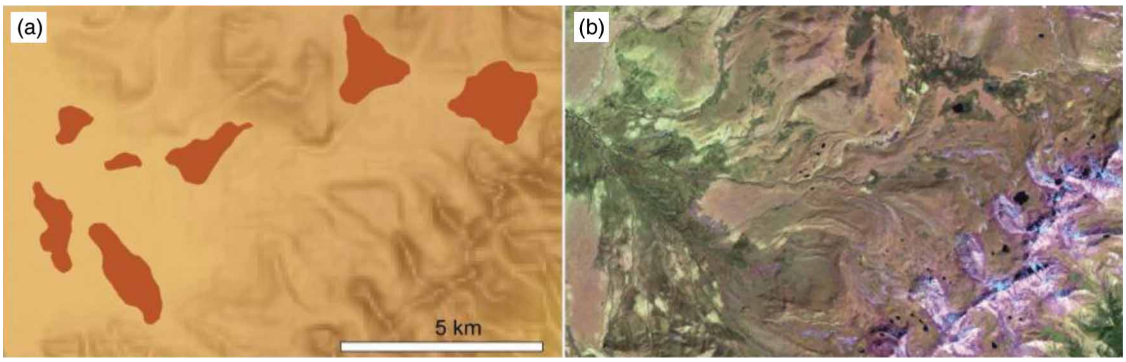

Figure 6. Examples of hummocky terrain (a) as mapped features on a DEM draped with a semi-transparent slope image, and (b) on Landsat imagery. Location of the area depicted is detailed in Figure 3.

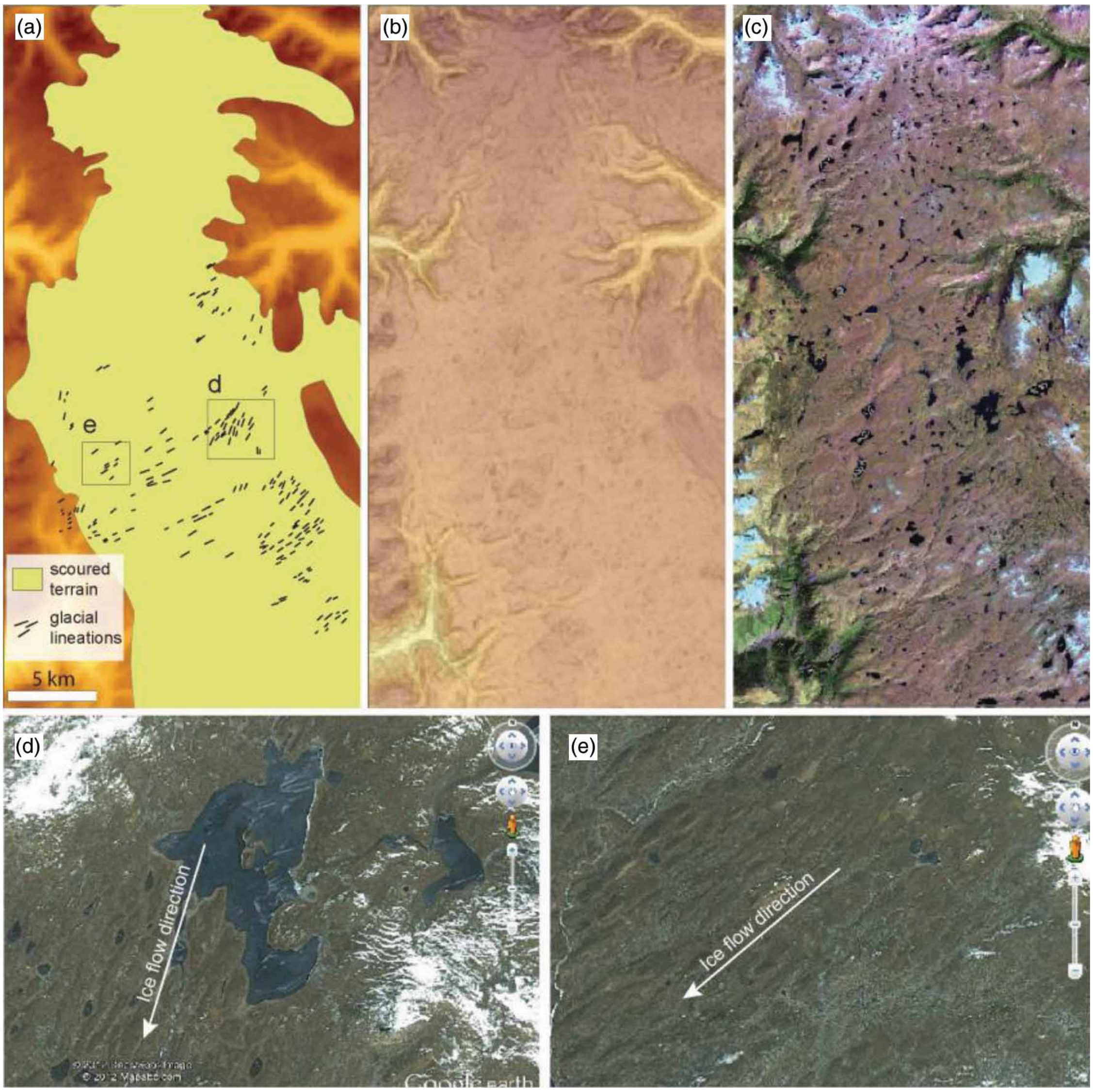

Figure 7. Examples of scoured terrain and glacial lineations (a) as mapped features, (b) on a DEM draped with a semi-transparent slope image, (c) and (d) on Landsat imagery, and (e) in Google Earth. Location of the area depicted in panels a–c is detailed in Figure 3. Locations for panels d and e occur in panel a.

and along valley sides, while elongated sinuous moraines only occur on the Haizishan plateau. Moraine length ranges from 10^2 to 10^4 meters. The longest sinuous moraine on the plateau surface can be traced for 50 km. Some moraines have clear, sharp crests while others are less distinct. A total of 593 marginal moraine polygons were mapped.

4.3 *Hummocky terrain*

Hummocky terrain is an irregular shaped sedimentary deposit of hills and mounds. The hummocky terrain mapped in the Shaluli Shan area are located along glacial valley sides, found crossing glacial valleys or extend beyond glacial valleys, in positions similar to that of the lateral or terminal moraines, indicating their glacial origin and therefore the position of the former glacier margin (Figure 6; Benn & Evans, 2010). There are a total of 38 hummocky terrain polygons mapped. They were mapped entirely from Landsat imagery and Google Earth, as they were difficult to identify from the 90 m DEM.

4.4 *Glacial lineations*

Glacial lineations are elongate features formed by subglacial streamlining, including both erosional and depositional processes. They occur in groups of subparallel ridges on the Haizishan and Xinlong plateaus. Many lineations were clustered in the central area of the Haizishan Plateau (Figure 2 and 7). Field inspection of the central area showed that lineations are moderately flat on top, wide, and that they probably consist of glacial till. The lineations located further away from the central area are slimmer and consist of till with a bedrock core. Some have asymmetric crag-and-tail long profiles. A total of 393 lineations were mapped with individual lengths from 70 m to 1000 m and widths from tens to more than 200 meters. Glacial lineations were mapped from Google Earth and Landsat imagery.

4.5 *Scoured terrain*

A landscape unit occurring on the Shaluli Shan, but largely absent in other areas of the Tibetan Plateau, is scoured terrain. Scoured terrain consists of low-relief bedrock-dominated surfaces with numerous rock basins and intervening rock knobs, typically resulting in a widespread occurrence of lakes (Figure 7). The two occurrences of terrain units cover areas of 465 km^2 and 753 km^2. We interpret the topography as formed by glacial plucking and abrasion. The widespread occurrence of glacial scouring indicates the presence of basal sliding with sheet flow style, warm-based ice. Boulders are widespread in the scoured area and marginal moraines and lineations overlap the scoured terrain, further strengthening the argument for its glacial origin.

5. Map quality and completeness

The map presents a detailed record of glacial landforms for the southeastern Tibetan Plateau. The entire map region has been thoroughly examined for glacial landforms in the DEM, satellite imagery, and Google Earth. The resolutions of the DEM and satellite imagery limit the size of detectable landforms so that those smaller than 70 meters have not been mapped, although they may exist. Field controls for selected key areas (Figure 3) confirm the mapped geomorphology.

6. Conclusions

Abundant glacial landforms in the Shaluli Shan, a currently largely ice free region on the Tibetan Plateau, indicate the former extent and style of past glaciations including large intermontane ice caps on the order of 10^3 km^2 and extensive valley glaciers. Landforms formed by valley glaciers are centered on high mountain ranges. Ice caps formed on large intermontane plateau surfaces created suites of landforms typical of warm-based ice such as scoured terrain, lineations and marginal moraines. The mapped glacial land-forms cover a total area of 1.65×10^4 km^2, which is the minimum extent of maximum glaciation.

Software

We used ERDAS Imagine 9.1 for processing the DEM and ENVI 3.4 for composing Landsat images. The mapping was performed using ArcGIS 9.3. Google Earth provided 3D visualization. Adobe Illustrator CS4 was used for producing the map.

Data

The author has supplied data (as an ESRI Shapefile) used in the production of the accompanying map. These are available as Supplementary Materials at http://dx.doi.org/10.1080/17445647.2012.668762. Whilst the contents of the ZIP file are the sole responsibility of the author, the journal has screened them for appropriateness.

Acknowledgements

We thank Emma Johansson, Jun Feng, Barbara Hauzenberger, Zhou Liping, and Björn Morén for discussions and fieldwork companionship. Funding for fieldwork and group workshops was provided by the Swedish Research Council/Swedish International Development Cooperation Agency (VR/SIDA) through their Swedish Research Links programme to Stroeven (No. 348-2007-6924).

References

Benn, B.D.I., & Evans, D.J.A. (2010). *Glaciers and glaciation* (2nd ed.). London: Elsevier.
Burchfiel, B.C., Chen, Z.L., Liu, Y.P., & Royden, L.H. (1995). Tectonics of the Longmen Shan and adjacent Regions, Central China. *International Geology Review*, *37*(8), 661–735, doi:10.1080/00206819509465424.
GLCF (2011). Global Land Cover Facility[Online]. Retrieved May 16, 2010, from http://www.landcover.org.
Graf, A.A., Strasky, S., Zhao, Z.Z., Akcar, N., Ivy-Ochs, S., Kubik, P.W., et al. (2008). Glacier extension on the eastern Tibetan Plateau in response to MIS 2 cooling, with a contribution to 10Be and 21Ne methodology. In S. Strasky (Ed.), *Glacial response to global climate changes: Cosmogenic nuclide chronologies from high and low latitudes* (pp. 77–110), PhD thesis, ETH Zürich.
Heyman, J., Hättestrand, C., & Stroeven, A.P. (2008). Glacial geomorphology of the Bayan Har sector of the NE Tibetan Plateau. *Journal of Maps*, *4,* 42–62, doi:10.4113/jom.2008.96.
Heyman, J., Stroeven, A.P., Alexanderson, H., Hättestrand, C., Harbor, J., Li, Y.K., et al. (2009). Paleoglaciation of Bayan Har Shan, northeastern Tibetan Plateau: Glacial geology indicates maximum extents limited to ice cap and ice field scales. *Journal of Quaternary Science*, *24,* 710–727, doi:10.1002/jqs.1305.
Heyman, J., Stroeven, A.P., Caffee, M.W., Hättestrand, C., Harbor, J., Li, Y.K., et al. (2011). Palaeoglaciology of Bayan Har Shan, NE Tibetan Plateau: Exposure ages reveal a missing LGM expansion. *Quaternary Science Reviews*, *30*(15–16), 1988–2001, doi:10.1016/j.quascirev.2011.05.002.
Jarvis, A., Reuter, H.I., Nelson, A., & Guevara, E. (2008). Hole-filled seamless SRTM data V4. International Centre for Tropical Agriculture (CIAT). Retrieved August 5, 2009, from http://srtm.csi.cgiar.org.
Kuhle, M. (1988). The Pleistocene glaciation of Tibet and the onset of ice ages - An autocycle hypothesis. *GeoJournal*, *17*(4), 581–595, doi:10.1007/BF00209444.
Lehmkuhl, F., & Owen, L.A. (2005). Late Quaternary glaciation of Tibet and the bordering mountains: A review. *Boreas*, *34*(2), 87–100, doi:10.1111/j.1502-3885.2005.tb01008.x.
Li, B.Y., Li, J.J., Cui, Z.J., Zheng, B.X., Zhang, Q.S., Wang, F.B., et al. (1991). Quaternary glacial dis- tribution map of Qinghai-Xizang (Tibet) plateau. Beijing: Science Press, Mapscale =1:3,000,000.
Morén, B., Heyman, J., & Stroeven, A.P. (2011). Glacial geomorpho- logy of the central Tibetan Plateau. *Journal of Maps*, *7,* 115–125, doi:10.4113/jom.2011.1161.
Owen, L.A., Finkel, R.C., Barnard, P.L., Ma, H.Z., Asahi, K., Caffee, M.W., et al. (2005). Climatic and topographic controls on the style and timing of Late Quaternary glaciation throughout Tibet and the Himalaya defined by 10Be cosmogenic radio-nuclide surface exposure dating. *Quaternary Science Reviews*, *24*(12–13), 1391–1411, doi:10.1016/j.quascirev.2004.10.014.
Rutter, N. (1995). Problematic ice sheets. *Quaternary International*, *28,* 19–37.
Schäfer, J.M., Tschudi, S., Zhao, Z., Wu, X., Ivy-Ochs, S., Wieler, R., et al. (2002). The limited influence of glaciations in Tibet on global climate over the past 170000 yr. *Earth and Planetary Science Letters*, *194*(3–4), 287–297.
Strasky, S., Graf, A.A., Zhao, Z., Kubik, P.W., Baur, H., Schlüchter, C., et al. (2009). Late Glacial ice advances in southeast Tibet. *Journal of Asian Earth Sciences*, *34*(3), 458–465, doi:10.1016/j.jseaes.2008.07.008.
Stroeven, A.P., Hättestrand, C., Heyman, J., Harbor, J., Li, Y.K., Zhou, L.P., et al. (2009). Landscape analysis of the Huang He headwa- ters, NE Tibetan Plateau - glacial and fluvial erosion patterns. *Geomorphology*, *103*(2), 212–226, doi:10.1016/j.geomorph.2008.04.024.
Wang, J., Raisbeck, G., Xu, X.B., Yiou, F., & Bai, S.B. (2006). *In situ* cosmo- genic 10Be dating of the Quaternary glaciations in the southern Shaluli Mountain on the southeastern Tibetan Plateau. *Science in China Series D: Earth Sciences*, *49*(12), 1291–1298, doi:10.1007/s11430-006-2026-5.
Xu, L.B., & Zhou, S.Z. (2009). Quaternary glaciations recorded by glacial and flu- vial landforms in the Shaluli Mountains, southeastern Tibetan Plateau. *Geomorphology*, *103,* 268–275, doi:10.1016/j.geomorph.2008.04.015.
Zheng, B.X., & Ma, Q.H. (1995). A study on the geomorphological characteristics and glaciations in Paleo-Daocheng Ice Cap, western Sichuan. *Journal of Glaciology and Geocryology*, *17,* 23–32, (In Chinese), doi:CNKI:SUN:BCDT.0.1995-01-003.
Zhou, S.Z., Li, J.J., Zhang, S.Q., Zhao, J.D., & Cui, J.X. (2004). Quaternary glaciations in China. In J. Ehlers & P.L. Gibbard (Eds.), *Quaternary glaciations extent and chronology, Part III: South America, Asia, Africa, Australasia, Antarctica* (pp. 105–113). Amsterdam: Elsevier.